Biosensors and Bioelectronics 77 (2016) 137–143

Contents lists available at ScienceDirect

Biosensors and Bioelectronics

journal homepage: www.elsevier.com/locate/bios

Rapid detection of multiple foodborne pathogens using a nanoparticle-functionalized multi-junction biosensor

Kara Yamada [a], Won Choi [a], Inae Lee [b], Byoung-Kwan Cho [c], Soojin Jun [a,*]

[a] Department of Human Nutrition, Food, and Animal Sciences, University of Hawaii, 1955 East-West Road, Honolulu, HI 96822, USA
[b] Department of Molecular Biosciences and Bioengineering, University of Hawaii, Honolulu, HI 96822, USA
[c] Department of Biosystems Machinery Engineering, Chungnam National University, Daejeon, South Korea

ARTICLE INFO

Article history:
Received 23 July 2015
Received in revised form
11 September 2015
Accepted 12 September 2015
Available online 14 September 2015

Keywords:
Multiplexing
Multi-function
Pathogens
Detection

ABSTRACT

Real-time identification of multiple bacterial pathogens in food is urgently needed to ensure food safety. Although rapid and sensitive detection methods offering simplicity, accuracy, and multiplexity are highly desirable for industrial food applications, the development of a biosensor that meets all criteria remains a challenge. In this study, a single walled carbon nanotube- (SWCNT) based multi-junction sensor was designed for potential multiplexed detection of foodborne pathogens. Gold tungsten wires (Ø: 50 μm) coated with polyethylenimine (PEI) and SWCNTs were aligned to form a 2×2 junction array, functionalized with streptavidin and biotinylated antibodies specific for *Escherichia coli* K-12 and *Staphylococcus aureus*. Electric current (I) measurements in response to target binding events in pure serial diluted samples of *E. coli* and *S. aureus* at each junction within the 2×2 array were monitored to create calibration curves. An inverse correlation between I signals and bacterial concentrations was observed. Changes in I (ΔI) were also calculated to reduce background noise and emphasize the SWCNT-based sensor's response to the biorecognition reactions between antibody and antigens. A linear regression was observed for both the *E. coli* and *S. aureus* functionalized array sensors, $R^2 = 0.978$ and $R^2 = 0.992$, in range of 10^2–10^5 CFU/mL. The calibration curves were used to evaluate the sensor's multiplexing capabilities to detect *E. coli* and *S. aureus* in 10 μL and 100 μL batch microbial cocktail samples.*I*signal responses exhibited similar measurement trends indicating that the developed SWCNT-based multi-junction biosensor has potential for sensitive, simple, and multiplexed applications.

Published by Elsevier B.V.

1. Introduction

Food safety monitoring is a key aspect within the food industry. The security and safety of our food depends on the ability to detect, identify and trace foodborne pathogens. However, minimizing the occurrence of microbial contamination remains a challenge due to the increase in production of minimally processed foods and the globalization of our food supply (Scallan et al., 2011). Potential biological threats to our health and economy emphasize the significance of foodborne pathogen detection methods. Despite greater biological understanding and technological advancements, current detection methods have significant drawbacks. Traditional plate counting, though accurate and affordable, is time-consuming and requires sample pre-enrichment. DNA amplification methods offer a faster detection time with good sensitivity, but are laborious and expensive; and magnetic-based approaches are applicable to complex food samples, but require lengthy sample preparation, costly reagents, and limited sensitivity (Kim et al., 2013). Furthermore, most methods involve the use of bench-top instruments in stationary laboratories operated by skilled personnel. Hence, development of an identification method that meets the requirements of miniaturization, cost-efficiency, and the ability for simultaneous detection of multiple analytes has become the key focus in the field of pathogen detection (Pedrero et al., 2009).

Biosensor technology offers promising solutions for portable, rapid and sensitive detection in food applications due to micro- and nano-fabrication techniques (Mello and Kubota, 2002). One of the advantages of applying micro- and nano-fabrication techniques into biosensors is the possibility of achieving multiplexed analysis within a shortened analysis time (Pedrero et al., 2009). Integration of nanomaterials into immunosensors has gained recognition for its ability to enhance bacterial detection. Engineered nanomaterials, such as magnetic nanoparticles (MNPs) (Varshney and Li, 2007; Ravindranath et al., 2009), carbon nanotubes (CNTs) (Chunglok et al., 2011; Zhao et al., 2011), nanorods (NRs) (Wang and Irudayaraj, 2008), quantum dots (QDs) (Zhao et al., 2009; Vinayaka and Thakur, 2010), and nanowires (NWs) (Wang et al.,

* Corresponding author. Fax: +1 808 956 4024.
E-mail address: soojin@hawaii.edu (S. Jun).

http://dx.doi.org/10.1016/j.bios.2015.09.030
0956-5663/Published by Elsevier B.V.

2008) have been used in biosensor research as catalytic tools, immobilization platforms and optical labels to improve sensitivity, stability and response time. Amongst the many nanomaterials, single-walled carbon nanotubes (SWCNTs) are a key focus in molecule-based electrical circuits and biosensor research based on their electrical, structural, and mechanical properties. The unique electrical properties of SWCNTs stem from the electronic structure of the two-dimensional (2-D) graphene sheet composed of a single atomic layer of graphite with a honeycomb lattice of sp^2 bonded carbon atoms (McEuen et al., 2002). Enhanced sensing performance can be attributed to SWCNTs' size compatibility to biomolecules, as they have the smallest diameter of 1 nm (Chen et al., 2003; Cherukuri et al., 2004; Barone et al., 2005). SWCNTs provide maximum interaction with adjacent biomolecules, in that all carbon atoms are in direct contact with its environment (Allen et al., 2007; Maroto et al., 2007; Heller et al., 2008). Thereby, electrochemical reactivity can be amplified, even at minute environmental variations (Wang, 2005; Vashist et al., 2011). In addition, the low charge carrier density of SWCNTs is comparable to the surface charge density of proteins, which makes SWCNTs well suited for electronic detection of target biomolecules (Heller et al., 2006). Therefore, when binding events occur at the SWCNT interface, the charge accumulation or depletion in the 1-D nanostructure takes place in the "bulk" of the structure, creating large electrical property changes that can potentially enable the detection of a single molecule (Wanekaya et al., 2006).

SWCNTs have been integrated into electrochemical immunosensors in field effect transistor (FET) designs (Besteman et al., 2003; Boussaad et al., 2003; Artyukhin et al., 2006) and for electrode surface modification as a means to improve electron transfer rates and working surface area (Okuno et al., 2007; Zhao et al., 2011). Studies have also used nanotubes to construct molecular junctions based on its ability to control the energy gap of electrons (Forzani et al., 2004; Aguilar et al., 2005; Maruccio et al., 2007). However, the intricate sensor designs and elaborate fabrication processes prevent SWCNT biosensors from evolving into practical sensing tools for industrial applications. A SWCNT-based biosensor with simple fabrication and minimal sensing procedures will offer an important step towards development of sensitive and selective bio-recognition devices for multiplexed foodborne pathogen detection.

In our previous study, the change in electrical current measurements of a SWCNT functionalized microwire single junction biosensor was monitored to detect *E. coli* at 10^2 CFU/mL with a detection time of less than 5 min (Yamada et al., 2014). Based on research findings, the objective was to incorporate SWCNTs into a multi-junction biosensing device for potential as a rapid sensing unit for portable multiplexed applications. The biosensor operates by optimizing a junction array with a bio-nano modified recognition platform to convert molecular binding events between target antigens and antibodies at each junction into measurable electrical signals used for pathogen identification and quantification.

2. Materials and methods

2.1. Materials

7% gold-tungsten plated wire (Ø: 50 μm) was manufactured from ESPI Metals (Ashland, OR). Polydimethylsiloxane (PDMS; Sylgard 184 silicone elastomer curing agent and base) was ordered through Dow Corning (Midland, MI). Copper clad printed circuit boards ($160.78 \times 114.30 \times 1.52$ mm^3) and etchant solutions were purchased from Radio Shack (Honolulu, HI). SWCNTs ($>95\%$ purity, Ø: 15 ± 5 nm, 1–5 μm lengths) were supplied from NanoLab, Inc. (Waltham, MA). Alcohol (95%), BD Bacto peptone, BBL trypticase soy broth and Difco plate count agar were procured from VWR (West Chester, PA). N,N-dimethylformamide (DMF), polyethylenimine (PEI, branched, average $M_w \sim 25{,}000$) and streptavidin from *Streptomyces avidinii* (affinity purified, lyophilized from 10 mM potassium phosphate, ≥ 13 U/mg protein) were purchased from Sigma Aldrich (St. Louis, MO). Biotinylated polyclonal *E. coli* (4 mg/mL) and *S. aureus* (4 mg/mL) antibodies and OXOID MacConkey agar were purchased from Thermo Fisher Scientific (Waltham, MA).

2.2. Instrumentation

Microwire sanitization and SWCNT dispersion were performed using a digital sonifier (450, Branson, Danbury, CT). An automated XYZ stage (Franklin Mechanical & Control Inc., Gilroy, CA) controlled by the COSMOS program (Velmex, Inc., Bloomfield, NY), furnace (Thermolyne, Thermo Scientific, Waltham, MA), and solder kit (Radio Shack, Honolulu, HI) were used during SWCNT coating and wire assembly. A desktop 3-D printer (TAZ 4, Lulz Bot, Loveland, CO) was used to fabricate the sensing device housing. Circuitry parts (Radio Shack, Honolul, HI) and picoammeter (6485, Keithley, Cleveland, Ohio) were integrated into the sensing system.

2.3. SWCNT coating technique

SWCNT networks can be formed by several approaches including spin coating and spray coating (Jang et al., 2008). Though spin coating is a simple method used to form SWCNT networks, it is limited to small planar areas and large amounts of SWCNT colloid solution are lost. In addition, spray coating, which is applicable to large surface areas, is not useful for obtaining uniform networks. To overcome these difficulties, the dip-coating method was used to coat the microwire electrodes.

SWCNTs were dispersed in DMF at a concentration of 0.1 g/L by sonicating the solution for 6 h (Rouse et al., 2004). After the initial 6 h of sonication, the dispersion was further sonicated for 2 h before use each day. Prior to SWCNT coating, microwire electrodes were cut to a length of 31 mm and sonicated in DI water, followed by 70% alcohol for 5 min each. Sanitized wires were dried in a furnace at 175 °C for 10 min and mounted onto the automated XYZ stage for step-wise surface modification. A computer was used to initiate the XYZ motor control program. Wires were immersed into glass vials containing 9 mL of 1% PEI solution for 5 min and withdrawn at a constant withdrawal velocity (ν_w) of 6 mm/min. PEI coated wires were baked at 175 °C for 1 h (Cairns, 2013). Subsequently, wires were re-mounted onto the XYZ stage and immersed into the SWCNT-DMF suspension for 5 min. The PEI coated wires were withdrawn at the same constant velocity ($\nu_w = 6$ mm/min) to generate a high capillary force and large influx of SWCNT colloids onto the wire (Jang et al., 2008). Dip coating into the SWCNT-DMF solution was repeated to achieve two dip coats, approximately 0.84 μm thick.

2.4. Device fabrication

Disposable sensor chips were fabricated as a base for the multi-junction arrays. Copper clad printed circuit (PC) boards were cut ($26 \times 26 \times 1.5$ mm^3), etched and cured with PDMS to form electrode connector pads and a PDMS sample well on each sensing chip (Fig. 1(a)). Four SWCNT coated wires were orthogonally placed and soldered to the connector pads to create a 2×2 junction array.

A multiplexing circuit, composed of a basic stamp 2 module (Parallax Inc.) with 20 MHz CPU speed and 32 bytes RAM, relay switches and a 1 V power source housed in a 3D printed box ($120 \times 92 \times 52$ mm), was connected to a picoammeter and

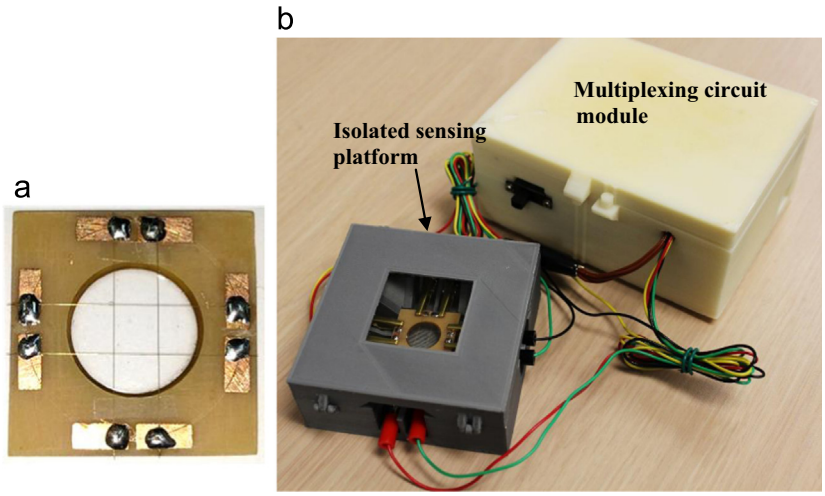

Fig. 1. Multi-junction sensor system. (a) Assembled multi-junction sensor chip. (b) 3-D printed multiplexing circuit module and sensing platform.

programmed to measure current at the four bio-nano junctions in real-time (Fig. 1(b)). A sensing platform ($80 \times 80 \times 30$ mm) with an acrylic observation window was also fabricated to provide a isolated sensing environment during current measurements.

2.5. Antibody immobilization

After SWCNT wire coating and junction assembly, antibodies were immobilized onto each junction to enhance sensor specificity. Self-assembled monolayers of streptavidin and biotinylated antibodies were formed on the SWCNT coated microwires (Lu and Jun, 2012). 5 μL of streptavidin was pipetted onto each junction. After 5 min, the droplet of streptavidin was removed. Subsequently, 5 μL of biotinylated antibodies (anti-*E. coli* or anti-*S. aureus*) was added to the junction for another 5 min, to form avidin-biotin complexes. Then, the droplet of biotinylated antibodies was removed and the functionalized bio-nano junction sensor was dried and ready for cell detection.

2.6. Microbial preparation

Frozen stock cultures of *E. coli* K-12 and *S. aureus* were obtained from the Food Microbiology collection, University of Hawaii. All experiments were conducted in a certified Biosafety Level II laboratory. 100 μL of each isolate was cultured separately in 10 mL of tryptic soy broth and incubated for 24 h at 37 °C to make a stock culture of each organism.

Test samples were prepared from serial dilutions of the stock cultures using 0.1% peptone water. The initial concentrations of *E. coli* and *S. aureus* stock cultures were obtained by plate counting methods on plate count agar. For microbial cocktails, a mixture of *E. coli* K-12 and *S. aureus* was prepared by centrifuging 1 mL of each stock culture at 2000 rpm for 15 min (Muhammad-Tahir and Alocilja, 2003). The resulting pellets were suspended in 0.1% peptone water to make a 10 mL solution. The microbial cocktail suspension was serially diluted in peptone water.

2.7. FESEM imaging

A field emission scanning electron microscope (FESEM) (Pacific Biosciences Research Center, University of Hawaii) was used to visualize the sensor's surface, after the capture of *E. coli* and *S. aureus* cells. Surface coating of the wires was required before loading the samples into the FESEM due to the nonconductive properties of bacteria. Each junction sample was attached to a conductive carbon tape adhered to an aluminum stub and pretreated in a Hummer 6.2 sputter coater for 45 s to achieve a thin layer of gold/palladium. Samples were then observed with a Hitachi S-4800 FESEM.

2.8. Multiplexing sensitivity tests

Each experiment was conducted in triplicate with 10 μL bacterial samples applied to each junction. The sensitivity of the multi-junction sensor was evaluated using pure serially diluted *E. coli* and *S. aureus* cultures. Anti- *E. coli* antibody functionalized multi-junction sensors were tested with 10^1–10^5 CFU/mL *E. coli* K-12 solutions. While, anti- *S. aureus* antibody functionalized sensors were tested with 10^1–10^5 CFU/mL *S. aureus*. The single analyte current measurements in response to the bacterial concentrations were used as calibration curves for the multi-analyte detection tests.

To evaluate the sensors' ability to simultaneously detect *E. coli* and *S. aureus*, each sensor chip was functionalized with both *E. coli* and *S. aureus* antibodies. The two top junctions of each sensor represented by $R_{1.1}$ and $R_{1.2}$ (Fig. 2(a)) were functionalized for *E. coli* detection and the bottom two junctions, $R_{2.1}$ and $R_{2.2}$, for *S. aureus* detection. As a preliminary multiplexed detection evaluation, 10 μL samples of mixed cultures of *E. coli* and *S. aureus* (10^1–10^5 CFU/mL) were applied to each junction and current values were measured. 100 μL batch samples were then applied to evaluate the multi-junction's batch sensing performance in larger volumes. Current measurements were compared to the calibration curves generated from the sensitivity tests.

2.9. Data measurement and analysis

To determine the sensitivity of the multi-junction array and calibrate the sensor for *E. coli* and *S. aureus* detection, the current (I) was measured at each of the four junctions and averaged together to obtain a representative I measurement for the sensing chip. Changes in current (ΔI) in response to *E. coli* and *S. aureus* binding events were calculated to minimize background noise, focusing on the sensor's ability to transduce biorecognition reactions into measurable signals. The ΔI signal response was determined by calculating the difference between the electrical current output of the negative control (I_{antibody}) and that of the sample ($I_{\text{antibody-bacteria}}$), as given by

$$\Delta I = \left| I_{(antibody-bacteria)} - I_{(antibody)} \right| \quad (1)$$

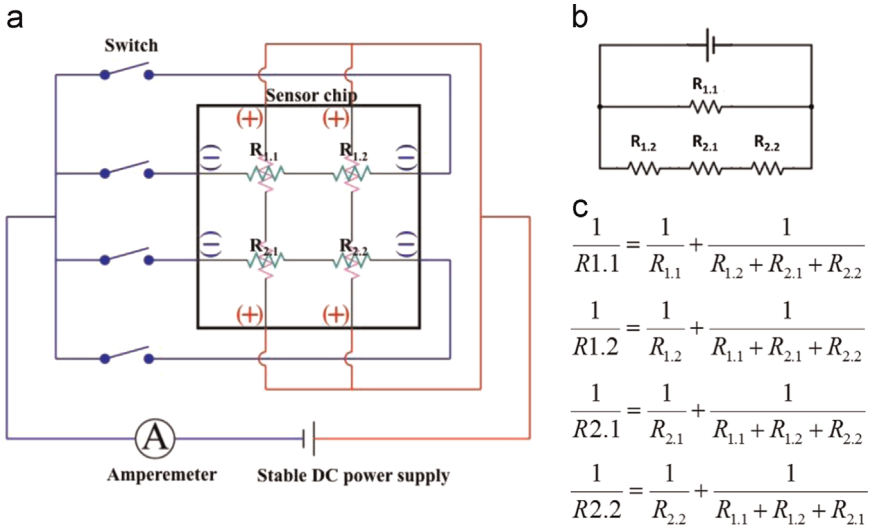

Fig. 2. (a) multiplexing multi-junction circuit composed of four relays, (b) electric current pathway and circuit equivalent at a single junction, and (c) mathematical equations used to calculate junction resistance.

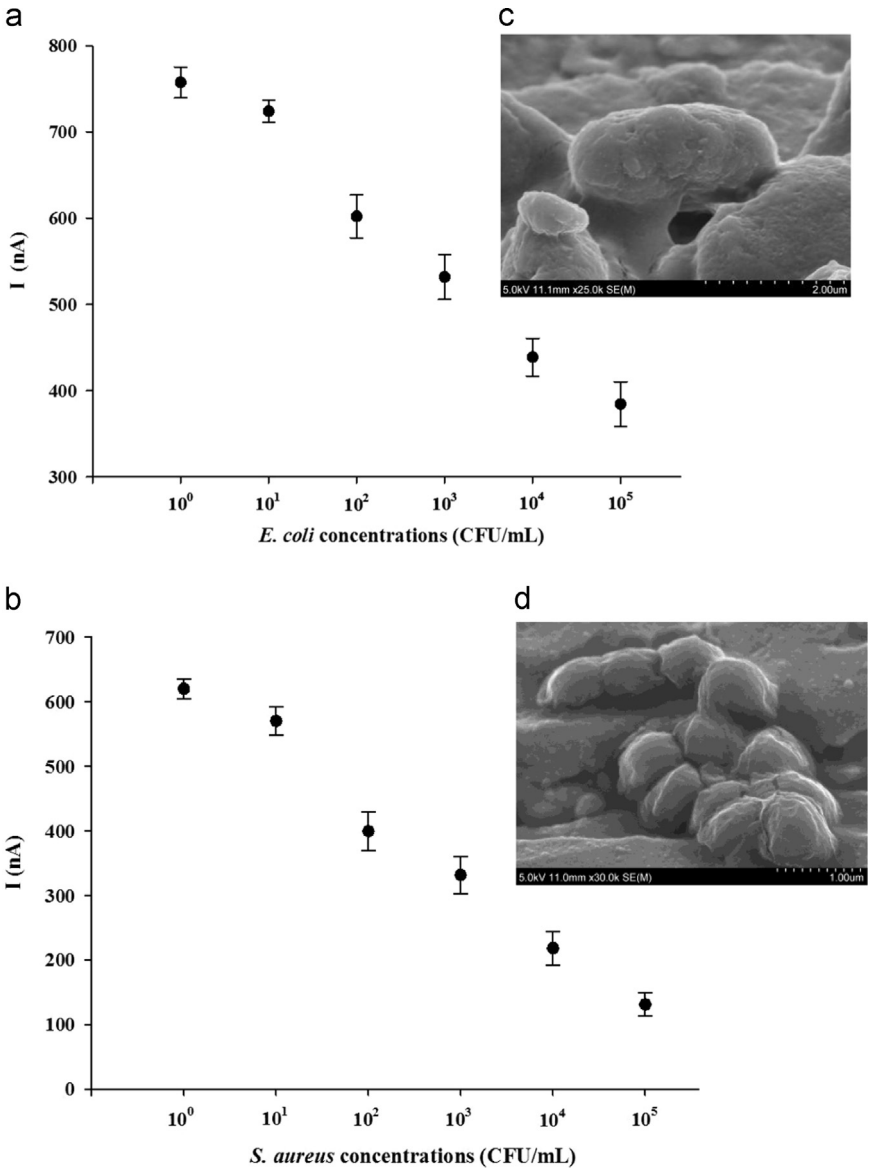

Fig. 3. Electrical current calibration curves for an anti-*E. coli* antibody (a) and an anti-*S. aureus* antibody (b) functionalized multi-junction sensor tested with a negative control (10^0 CFU/mL) and both bacteria in the range of 10^1–10^5 CFU/mL. SEM images of *E. coli* cells (c) and *S. aureus* cells (d) bound to sensor surface.

Standard deviations of the current changes were expressed as error bars in the corresponding graphs.

To determine the multiplexing capability of the sensor to simultaneously detect *E. coli* and *S. aureus* in a mixed sample, *I* measurements from the anti-*E. coli* functionalized junctions, $R_{1.1}$ and $R_{1.2}$, and anti-*S. aureus* junctions, $R_{2.1}$ and $R_{2.2}$, were averaged and compared to the calibration curves.

A mathematical equation was also built to calculate the resistance at each junction ($R_{1.1}$, $R_{1.2}$, $R_{2.1}$, and $R_{2.2}$), based on the assumption that as bacterial cells bind to each junction, all four junctions become interrelated (Fig. 2(b)). The Jacobian matrix method was selected as the numerical method to solve the non-linear simultaneous equations (Fig. 2(c)). The second order, non-linear simultaneous equations were solved by Mathematica software (Wolfram Research, Champaign, IL). The experimental *I* values were used in the equations to calculate the resistance of each junction. The calculated resistances of the sensor tested with pure and microbial cocktails were compared.

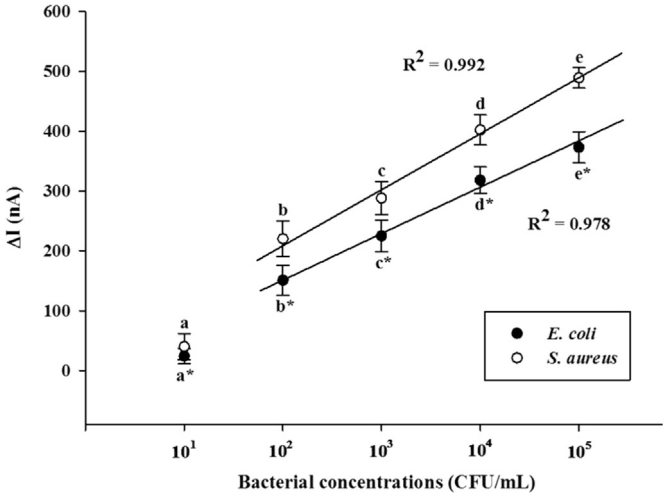

Fig. 4. Relationship between changes in current and concentrations of *E. coli* and *S. aureus* from 10^1 to 10^5 CFU/mL. Average signals (current drop) with different superscripts are significantly different at 95% confidence level (probability < 0.05). **E. coli* and *S. aureus* ΔI values were analyzed separately. ΔI was calculated using Eq. (1).

3. Results and discussion

3.1. Sensitivity tests for E. coli K-12 and S. aureus

The multi-junction array sensor was functionalized with anti-*E. coli* antibodies and tested with pure *E. coli* K-12 concentrations from 10^1 to 10^5 CFU/mL. The averaged current values of the sensor were used to create an *E. coli* calibration curve (Fig. 3(a)). The current decreased as the *E. coli* concentration increased. When no bacteria were present (control) the current value was 757 ± 13 nA. Once *E. coli* was added to the junctions, antigen–antibody reactions occurred on the bio-nano modified junction surface (Fig. 3(c)), changing the SWCNT morphology and altering its electrical properties. The current reduced to 384 ± 36 nA in a high concentration of *E. coli*, 10^5 CFU/mL. The control measurements confirmed that the responses were caused exclusively by the binding between *E. coli* and the antibody and the subsequent transduction of the SWCNT layer.

The same trend was observed with the anti- *S. aureus* functionalized sensor tested in pure *S. aureus* concentrations, but on a different current scale. A drop in current was measured from 620 ± 15 nA (control) to 131 ± 18 nA, respectively, as *S. aureus* cells (10^1–10^5 CFU/mL) were captured on the sensor (Fig. 3(b) and (d)). This suggested that the multi-junction sensor is capable of detecting *E. coli* and *S. aureus* simultaneously in a mixed bacterial solution, since the current signals vary depending on the target analyte and antibody. For example, a 10^3 CFU/mL concentration of *E. coli* detected on *E. coli* specific junctions had an averaged current signal of 532 ± 22 nA, while the same concentration of *S. aureus* detected with *S. aureus* specific junctions generated a current of 332 ± 28 nA. A similar current trend was observed in Fernandes et al., (2014) study, in which *E. coli* O157:H7 cells detected on a nanoparticle-based DNA electrochemical biosensor exhibited higher current values than *S. aureus* of the same concentration.

To highlight the sensor's ability to transduce the biorecognition reactions between antibody and antigen into measurable signals, the ΔI was calculated for *E. coli* and *S. aureus* sensors in range of 10^1–10^5 CFU/mL using Eq. (1) (Fig. 4). As bacterial concentrations increased, a greater change in current was measured proportional to the drop in current. The *E. coli* sensor's ΔI ranged from 24 to 373 nA, whereas, the *S. aureus* sensor's ΔI varied from 40 to 489 nA. A linear regression was observed for both the *E. coli* and *S. aureus* functionalized array sensors, $R^2 = 0.978$ and $R^2 = 0.992$, in range of 10^2–10^5 CFU/mL.

The multi-junction sensor's ΔI values for the 10^2 CFU/mL samples for both *E. coli* and *S. aureus* were significantly different from the values at 10^1 CFU/mL. The design of the 2×2 junction array was able to achieve a detection limit of 10^2 CFU/mL with a detection time of 1 min. In addition, the magnitude of the ΔI differed between the two bacterial strains, suggesting that multiplexed detection in samples contained various pathogens is possible.

3.2. Simultaneous detection of E. coli and S. aureus

To explore the response of the multi-junction sensor for simultaneous bacterial detection, mixed samples of *E. coli* and *S. aureus* were tested. Current responses from batch mixed samples, when 10 μL volume samples were pipetted on each junction and 100 μL samples covered all four junctions, were analyzed. Current measurement values corresponding to simultaneous *E. coli* and *S. aureus* detection demonstrated the same trend observed when pure microbial samples were applied (Fig. 5).

Current responses from the individual 10 μL multi-analyte samples applied to each junction closely paired with the calibration values. Measurements from the larger sample volume of 100 μL also exhibited similar trends. Data suggests that there is potential for multiplexed batch detection of pathogens when selective antibodies are used, in that the multi-junction's sensing performance was not compromised despite the presence of multiple analytes.

3.3. Mathematical circuit for multi-junction resistance calculation

A mathematical circuit equation was designed to calculate the resistance at each junction. Based on the assumption that all four junctions are connected to each other when bacterial samples are applied, the current measurement at one junction may be affected by the biorecognition events occurring at the other three junctions. Therefore, the equivalent circuit equations were used to determine the resistance at the specific junction without the bias from the other junctions. Experimental current values measured at the four junctions were inputted into the second order non-linear simultaneous equations. The calculated resistance values of top ($R_{1.1}$ and $R_{1.2}$) and bottom ($R_{2.1}$ and $R_{2.2}$) junctions were averaged to represent the resistance for *E. coli* and *S. aureus*, respectively (Table 1). The averaged resistance for *E. coli* and *S. aureus* detected in single and multi-analyte (10 μL) samples were compared.

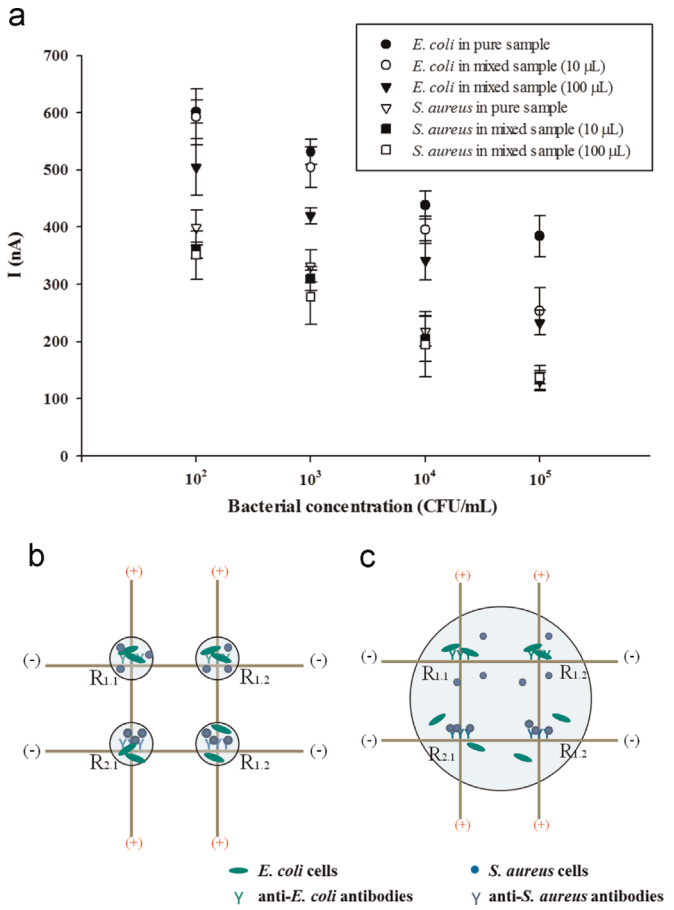

Fig. 5. (a) Current measurements for simultaneous detection of *E. coli* and *S. aureus* in 10 and 100 μL samples in comparison to calibration measurements. The bottom schematic illustrations show batch-type multiplexing tests using (b) 10 μL microbial cocktail samples of *E. coli* and *S. aureus* applied to **each junction** and (c) 100 μL samples applied to cover **all four junctions**.

Table 1
Multi-junction sensing array resistance calculated using the developed mathematical circuit.

Concentration (CFU/mL)	Analyte detection	Resistance (10^{-3} Ω)	
		E. coli: Averaged $R_{1.1}$ *and* $R_{1.2}$	*S. aureus*: Averaged $R_{2.1}$ and $R_{2.2}$
10^2	Single	2.15 ± 0.07^{a}	$3.56 \pm 0.13^{a*}$
	Mixed	2.14 ± 0.04^{a}	$3.70 \pm 0.06^{a*}$
10^3	Single	2.36 ± 0.08^{b}	$4.10 \pm 0.10^{b*}$
	Mixed	2.35 ± 0.05^{b}	$4.21 \pm 0.09^{b*}$
10^4	Single	2.59 ± 0.06^{c}	$5.19 \pm 0.08^{c*}$
	Mixed	2.73 ± 0.21^{c}	$5.17 \pm 0.06^{c*}$
10^5	Single	2.80 ± 0.05^{c}	$7.04 \pm 0.06^{d*}$
	Mixed	3.44 ± 0.02^{d}	$6.96 \pm 0.10^{d*}$

Significant differences for resistance values of E. coli and S. aureus were indicated by letters without and with the symbol of '*'.

The resistances obtained for the multi-junction sensor tested in the single analyte bacterial samples were in good agreement with the values calculated from the multi-analyte samples, as there were no significant differences between the samples in range of 10^2–10^4 CFU/mL for *E. coli* detection and 10^2–10^5 CFU/mL for *S. aureus* detection. A significant difference was observed between the single and mixed *E. coli* 10^5 CFU/mL measurements, which may have been due to non-specific binding (Radke and Alocilja, 2005). In addition, the resistance values increased from 10^2–10^5 CFU/mL and corresponded to the experimental current data trend, as resistance is inversely related to current. Increased bacteria cell binding at the junctions serve as an insulating material, thus altering the interfacial electron transfer at the junctions and modulating the electrical properties of the SWCNT sensing platform.

4. Conclusion

The incorporation of immobilized antibodies and a SWCNT-modified sensing platform into a disposable, label-free bio-nano functionalized junction sensor shows great promise for the detection of bacteria in serially diluted cultures. The multi-junction device demonstrates potential as a portable and affordable system composed of a multiplexing circuit module, isolated sensing platform, and multi-junction array chip. Testing the 2×2 multi-junction array with pure and mixed *E. coli* and *S. aureus* concentrations achieved batch-type multiplexed detection down to 10^2 CFU/mL. A linear regression with an $R^2 = 0.978$ was observed for *E. coli* and $R^2 = 0.992$ for *S. aureus* functionalized array sensors, in range of 10^2–10^5 CFU/mL. Microbial cocktail samples of *E. coli* and *S. aureus* showed similar measurement trends for multiplexed detection in 10 μL and 100 μL batch samples.

The SWCNT-based biosensor represents the first step toward developing a bio-nano junction sensing array for simultaneous detection of multiple pathogens. By offering simplicity, portability, and rapid detection, this biosensor shows promise as a field-deployable system for food and agricultural applications. Future studies will consider the evaluation of the developed sensor with food samples as well as bacterial cell concentration methods to further improve the limit of detection.

Acknowledgment

This study was completed with partial support of the MSIP (Ministry of Science, ICT & Future Planning in Korea). The authors would like to acknowledge Dr. Yong Li for kindly providing the bacterial strains and the use of his Food Microbiology Lab, and Dr. Marilyn F. Dunlap and Tina M. Carvalho for use their Biological Electron Microscope Facility.

References

Aguilar, A.D., Foranzi, E.S., Li, X., Tao, N., Nagahara, L.A., Amlani, I., Tsui, R., 2005. Appl. Phys. Lett. 87, 193108-1–193108-3.
Allen, B.L., Kichambare, P.D., Star, A., 2007. Adv. Mater. 19, 1439–1451.
Artyukhin, A.B., Stagermann, M., Friddle, R.W., Stroeve, P., Bakajin, O., Noy, A., 2006. Nano Lett. 6, 2080–2085.
Barone, P.W., Baik, S., Heller, D.A., Strano, M.S., 2005. Nat. Mater. 4 86-U16.
Besteman, K., Lee, J., Wiertz, F.G.M., Heering, H.A., Dekker, C., 2003. Nano Lett. 3, 727–730.
Boussaad, S., Tap, N.J., Zhang, R., Hopson, T., Nagahara, L.A., 2003. Chem. Commun. 13, 1502–1503.
Cairns, A., 2013. Optimization study of polyethyleneimine surface coating for microtip DNA Purification, Doctoral dissertation. University of Washington.
Chen, R.J., Bangsaruntip, S., Drouvalakis, K.A., Kam, N.W.S., Shim, M., Li, Y.M., Kim, W., Utz, P.J., Dai, H., 2003. Proc. Natl. Acad. Sci. USA 100, 4984–4989.
Cherukuri, P., Bachilo, S.M., Litovsky, S.H., Weisman, R.B., 2004. J. Am. Chem. Soc. 126, 15638–15639.
Chunglok, W., Wuragil, D.K., Oaew, S., Somasundrum, M., Surareungchai, W., 2011. Biosens. Bioelectron. 26, 3584–3589.
Fernandes, A.M., Zhang, F., Sun, X., 2014. Int. J. Curr. Microbiol. Appl. Sci. 3, 750–759.
Forzani, E.S., Zhang, H.Q., Nagahara, L.A., Amlani, I., Tsui, R., Tao, N., 2004. Nano Lett. 4, 1785–1788.
Heller, I., Janssens, A.M., Mannik, J., Minot, E.D., Lemay, S.G., Dekker, C., 2008. Nano Lett. 8, 591–595.
Heller, I., Kong, J., Williams, K.A., Dekker, C., Lemay, S.G., 2006. J. Am. Chem. Soc. 128, 7353–7359.

Jang, E.Y., Kang, T.J., Im, H.W., Kim, D.W., Kim, Y.H., 2008. Small 4, 2255–2261.
Kim, J.-H., Hiraiwa, M., Lee, H.-B., Lee, K.-H., Cangelosi, G.A., Chung, J.-H., 2013. RSC Adv. 13, 4281–4287.
Lu, L., Jun, S., 2012. Biosens. Bioelectron. 36, 257–261.
Maroto, A., Balasubramanian, K., Burghard, M., Kern, K., 2007. Chemphyschem 8, 220–223.
Maruccio, G., Marzo, P., Krahne, R., Passaseo, A., Cingolani, R., Rinaldi, R., 2007. Small 3, 1184–1188.
McEuen, P.L., Fuhrer, M., Park, H., 2002. IEEE Trans. Nanotechnol. 1, 78–85.
Mello, L.D., Kubota, L.T., 2002. Food Chem. 77, 237–256.
Muhammad-Tahir, Z., Alocilja, E.C., 2003. Biosens. Bioelectron. 18, 813–819.
Okuno, J., Maehashi, K., Kerman, K., Takamura, Y., Matsumoto, K., Tamiya, E., 2007. Biosens. Bioelectron. 22, 2377–2381.
Pedrero, M., Campuzano, S., Pingarrón, J.M., 2009. Sensors 9, 5503–5520.
Radke, S.M., Alocilja, E.C., 2005. IEEE Sens. J. 5, 744–750.
Ravindranath, S.P., Mauer, L.J., Deb-Roy, C., Irudayaraj, J., 2009. Anal. Chem. 81, 2840–2846.
Rouse, J.H., Lillehei, P.T., Sanderson, J., Siochi, E.J., 2004. Chem. Mater. 16, 3904–3910.
Scallan, E., Hoekstra, R.M., Angulo, F.J., Tauxe, R.V., Hoekstra, R.M., 2011. Emerg. Infect. Dis. 17, 7–16.
Varshney, M., Li, Y., 2007. Biosens. Bioelectron. 22, 2408–2414.
Vashist, S.K., Zheng, D., Al-Rubeaan, K., Luong, J.H.T., Sheu, F., 2011. Biotechnol. Adv. 29, 169–188.
Vinayaka, A.C., Thakur, M.S., 2010. Anal. Bioanal. Chem. 397, 1445–1455.
Wanekaya, A.K., Chen, W., Myung, N.V., Mulchandani, A., 2006. Electroanalysis 18, 533–550.
Wang, C., Irudayaraj, J., 2008. Small 4, 2204–2208.
Wang, J., 2005. Electroanalysis 17, 7–14.
Wang, R., Ruan, C., Kanayeva, D., Lassiter, K., Li, Y., 2008. Nano Lett. 8, 2625–2631.
Yamada, K., Kim, C.-T., Kim, J.-H., Chung, J.-H., Lee, H.G., Jun, S., 2014. Plos One 9 (9), e 105767.
Zhao, G., Zhan, Z., Dou, W., 2011. Anal. Biochem. 408, 53–58.
Zhao, Y., Ye, M., Chao, Q., Jia, N., Ge, Y., Shen, H., 2009. J Agric Food Chem. 57, 517–524.